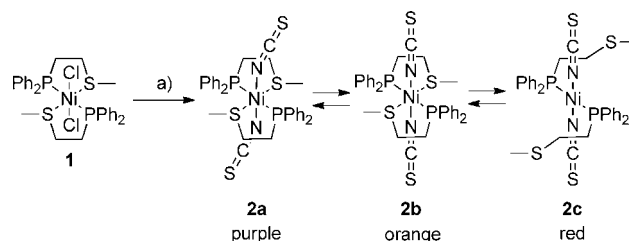


# Crystallographic Snapshots of the Bond-Breaking Isomerization Reactions Involving Nickel(II) Complexes with Hemilabile Ligands\*\*

Charles W. Machan, Alejo M. Lifschitz, Charlotte L. Stern, Amy A. Sarjeant, and Chad A. Mirkin\*

Hemilabile ligands have been used to prepare a wide variety of complexes, which are important in many fields ranging from catalysis to biomimetic chemistry.<sup>[1–5]</sup> These ligands allow coordination complexes to be prepared where one end of the hemilabile ligand is anchored to a metal center, while the other often is involved in fluxional processes. Indeed, in certain cases, researchers refer to these structures as “windshield-wiper” ligands,<sup>[6–9]</sup> since the weakly binding portion of the ligand can often dissociate and re-coordinate to the metal center, undergoing exchange in the presence of a coordinating solvent. Consequently, many researchers employ hemilabile ligands to stabilize what effectively are highly reactive solvent adducts or coordinatively unsaturated species.<sup>[10–20]</sup> As a result, complexes with certain types of hemilabile ligands have been made and characterized in both monodentate and multidentate states with different ancillary ligands.<sup>[21–26]</sup> To our knowledge, however, there is no example where a pair of isomeric structures, which represent the two “end states” that define a hemilabile ligand exchange process (where no displacement reaction has taken place), have been crystallographically characterized. The reason for this observation is that invariably in such systems one state is significantly more stable than the other in a given environment, or the exchange process occurs dynamically under rapid exchange conditions and the identities of the complexes exchanging can only be inferred through in situ spectroscopic means. Herein, we report the synthesis, isolation, and crystallographic characterization of a series of octahedral and square planar structurally isomeric nickel(II) complexes **2a–2c**,<sup>[27]</sup> which effectively define the two key “end states” in a well-defined bond-breaking isomerization reaction and a likely intermediate complex. While these structures are stable in the solid state, they rapidly interconvert in solution at room temperature.

The reaction of complex **1** with two equivalents of sodium thiocyanate (NaSCN) in a mixture of CH<sub>2</sub>Cl<sub>2</sub> and EtOH yields a mixture of complexes **2a–2c** (Scheme 1). In solution at room temperature, these complexes are rapidly intercon-



**Scheme 1.** Synthesis of complexes **2a–c**. a) 2 equiv NaSCN in 1:1 CH<sub>2</sub>Cl<sub>2</sub>/EtOH for 1 h.

verting, as evidenced by a single broad <sup>31</sup>P{<sup>1</sup>H} NMR resonance observed at  $\delta = 32.6$  in CD<sub>2</sub>Cl<sub>2</sub>. Variable-temperature (VT) <sup>31</sup>P{<sup>1</sup>H} NMR spectroscopy confirmed that this broadening is a result of rapid exchange between multiple complexes. When the temperature of the solution was lowered to 213 K in a stepwise manner, the spectrum changed significantly. At 238 K, a sharp resonance at  $\delta = 32.6$  ppm assigned to **2a** is observed along with a broad one at  $\delta = 8.7$  ppm assigned to **2c** (Supporting Information, Figure S1). The assignments for these resonances are based upon literature precedent<sup>[28,29]</sup> involving model complexes and crystallographic data (see below).

Interestingly, when red-orange CH<sub>2</sub>Cl<sub>2</sub> solutions containing these rapidly interconverting complexes were layered with diethyl ether, both purple and orange block-like crystals formed, along with red plates. Single-crystal X-ray diffraction studies of the purple, orange, and red crystals showed that they were **2a**, **2b**, and **2c**, respectively (Figure 1).<sup>[30]</sup> The structure of **2a** consists of a nickel(II) center in an octahedral geometry, defined by two chelating P,S–Me ligands coordinated in a *trans* configuration to form the equatorial plane. Furthermore, it has two apical nitrogen-bound SCN<sup>–</sup> ligands, which are bent relative to the equatorial plane (150–160°; Figure 1a and Supporting Information, Table S1). The struc-

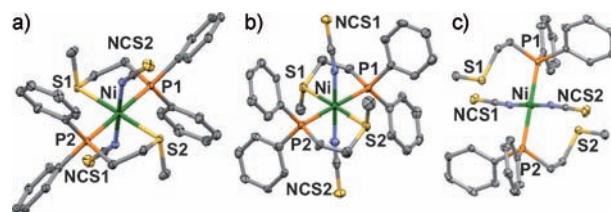


**Figure 1.** X-ray crystallographically determined structures for complexes **2a** (a), **2b** (b), and **2c** (c). Ni green, C gray, P orange, N blue, S yellow. Ellipsoids set at 50% probability; hydrogen atoms omitted for clarity.

[\*] C. W. Machan, A. M. Lifschitz, C. L. Stern, Dr. A. A. Sarjeant, Prof. Dr. C. A. Mirkin  
Department of Chemistry, Northwestern University  
2145 Sheridan Rd, Evanston, IL 60208 (USA)  
E-mail: chadnano@northwestern.edu  
Homepage: <http://chemgroups.northwestern.edu/mirkingroup/>

[\*\*] We thank Northwestern IMSERC for analytical instrumentation. We are grateful to Prof. Dr. Gregory L. Hillhouse for helpful suggestions concerning this manuscript. C.A.M. is grateful to NSF, ARO, and AFOSR-MURI for generous funding.

Supporting information for this article is available on the WWW under <http://dx.doi.org/10.1002/ange.201107620>.

ture of **2b** is nearly identical to complex **2a**, with the exception of the orientation of the apical  $\text{SCN}^-$  ligands, which are bound to nickel perpendicular to the equatorial plane formed by the P,S chelates (ca.  $170^\circ$ , Figure 1b). The structure of **2c** is square planar in geometry around the nickel center with two monodentate P,S–Me ligands (bound only through P) and two nitrogen-bound  $\text{SCN}^-$  ligands in a near-linear configuration with nickel (ca.  $170^\circ$ ; Figure 1c, Supporting Information, Table S1).

Polymorphism, linkage isomerism, and the ability of coordination complexes to crystallize as different geometric isomers under identical conditions have been reported previously,<sup>[21,23–26]</sup> but to our knowledge there are no examples of the solid-state characterization of some of the key participants in a hemilabile ligand exchange process, especially the dissociated state where no displacement reaction by solvent molecule or coordinating ligand has taken place. These structures are most aptly described as “bond-breakage isomers” rather than polymorphs. The observation of their existence is also dissimilar to bond-stretch isomerism, since the complexes in question (**2a**, **2b**, and **2c**) differ in ligand–metal connectivity.<sup>[22,25b,31,32]</sup> Linkage isomerism can also result in isomerization reactions that may be characterized in the solid state, but these products differ in ligand connectivity and not coordination number.<sup>[26]</sup> The fact that these crystal structures have “open” and “closed” coordination sites under the same solvent conditions lends credence to the conclusion that they represent crystallographic snapshots of an in situ bond-breaking isomerization reaction (see below).

To fully characterize this system, we studied the crystalline products by FTIR spectroscopy, focusing on the  $\text{SCN}^-$  regions since this functional group exhibits highly diagnostic stretches dependent upon coordination mode to the metal center.<sup>[33]</sup> Interestingly, examination of the bulk powder consisting of **2a–c** with an optical microscope shows a microcrystalline powder that contains the same three crystal types obtained by solvent layering (Supporting Information, Figure S2), with the majority product being **2a**. Owing to difficulties associated with the mechanical separation of **2c** from the other components of this mixture (**2a** and **2b**), we were unable to isolate adequate quantities of **2c** for study by FTIR spectroscopy. Since we could obtain macroscopic quantities of crystals of pure **2a** and **2b**, respectively, we could measure their FTIR spectra. Each exhibits a  $\nu_{\text{CN}}$  stretch diagnostic of non-bridging N-bound thiocyanate (Supporting Information, Figure S3, Table S2).<sup>[33,34]</sup> Importantly, when these crystals of **2a** or **2b** were dissolved in  $\text{CD}_2\text{Cl}_2$  and characterized by  $^{31}\text{P}\{^1\text{H}\}$  NMR spectroscopy, only a single broad resonance at  $\delta = 32.6$  ppm was observed, which is consistent with the  $^{31}\text{P}\{^1\text{H}\}$  NMR data for the mixture of isomers in solution. Based on the characterization of three distinct isomers in the solid state, we decided to determine if the three structures exist in solution as well. To do so, it was necessary to synthesize two analogue complexes, **4a** and **4b**, which have weakly chelating and non-chelating phosphine ligands, respectively, and can provide representative and meaningful comparative spectroscopic data (see Scheme 2). Since substitution of the methyl group on the thioether with a phenyl ring reduces the electron

richness of the thioether,<sup>[6]</sup> this ligand should favor an “open” monodentate coordination mode. Indeed, complex **4a** was synthesized from a complex (**3a**) prepared from  $\text{NiCl}_2 \cdot 6\text{H}_2\text{O}$  and two equivalents of  $\text{Ph}_2\text{PCH}_2\text{CH}_2\text{SPh}$  under similar conditions to those used to prepare **2a–c** (see the Supporting Information). As well as being characterized in the solid state by a single-crystal X-ray diffraction study (Figure 2a), **4a** was characterized in solution by  $^{31}\text{P}\{^1\text{H}\}$ ,  $^1\text{H}$ , and  $^{13}\text{C}\{^1\text{H}\}$  NMR spectroscopy.<sup>[30]</sup> All data are consistent with the solution and solid-state structures being very similar.<sup>[28,29]</sup>

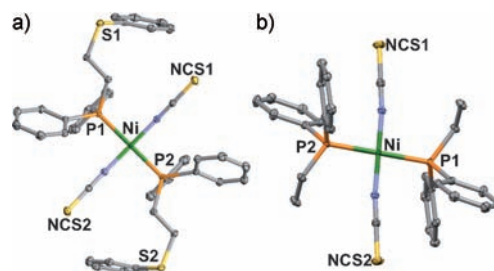
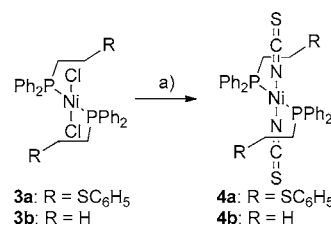


**Figure 2.** X-ray crystallographically determined structures for complexes **4a** (a) and **4b** (b). Ni green, C gray, P orange, N blue, S yellow. Ellipsoids set at 50% probability; hydrogen atoms omitted for clarity.

The solid-state structure of **4a** consists of a square-planar nickel center with two equivalents of N-bound  $\text{SCN}^-$  ligands and two equivalents of P-bound monodentate P,S–Ph ligands arranged in *trans* configurations. Importantly, the room temperature  $^{31}\text{P}\{^1\text{H}\}$  NMR spectrum of **4a** in  $\text{CD}_2\text{Cl}_2$  exhibits a broad resonance at  $\delta = 10.9$  ppm, which sharpens with decreasing temperature (Supporting Information, Figure S1B), consistent with a monodentate coordination mode for the phosphine ligand.<sup>[28]</sup> Similarly, model compound **4b**, which contains a non-chelating phosphine ligand, was synthesized from complex **3b** under nearly identical chloride abstraction conditions to those used for **3a** (see the Supporting Information; Scheme 2, Figure 2a). As in the case of **4a**, a single-crystal X-ray diffraction study of **4b** and  $^{31}\text{P}\{^1\text{H}\}$ ,  $^1\text{H}$ , and  $^{13}\text{C}\{^1\text{H}\}$  NMR spectroscopy indicated similar structures in solution and the solid state (Figure 2b).<sup>[30]</sup> The solid-state structure of **4b** showed a square-planar nickel center, much like **4a**, with two equivalents of N-bound  $\text{SCN}^-$  ligands and two equivalents of the non-chelating phosphine each arranged in a *trans* configuration. Significantly, room-temperature  $^{31}\text{P}\{^1\text{H}\}$  NMR spectroscopy of **4b** in  $\text{CD}_2\text{Cl}_2$  showed a single sharp resonance at  $\delta = 16.7$  ppm that remains unchanged with decreasing temperature. This complex,



**Scheme 2.** Synthesis of complexes **4a** and **4b** from **3a** and **3b**. a) 2 equiv NaSCN in 1:1  $\text{CH}_2\text{Cl}_2/\text{EtOH}$  for 1 h.

which does not have thioethers, does not undergo the fluxional exchange processes observed with **4a** and **2a–c**. The chemical shift of the resonance is similar to that observed for **4a**, consistent with the assignment of this complex as one with monodentate phosphinoalkylthioether ligands (Supporting Information, Figure S1B). Based on the spectroscopic data of model complex **4a**, we assign the  $^{31}\text{P}\{^1\text{H}\}$  NMR resonance observed at  $\delta = 8.7$  ppm in the mixture of **2a–c** at low temperature in  $\text{CD}_2\text{Cl}_2$  to the “open structure” **2c**. Compound **1** (which has two chloride ligands) serves as a model complex for octahedral compounds with *trans* phosphine and *trans* thioether ligands, such as **2a** and **2b**. Indeed, in  $\text{CD}_2\text{Cl}_2$ , complex **1**<sup>[29]</sup> exhibits a downfield resonance at  $\delta = 32$  ppm in its  $^{31}\text{P}\{^1\text{H}\}$  NMR spectrum, which is highly diagnostic of structures with five-membered P-containing chelates and remarkably close to the second resonance at  $\delta = 32.6$  ppm observed for the mixture of **2a–c** at low temperature.<sup>[28]</sup> We have not observed a third resonance at low temperature, and therefore speculate that **2a** and **2b** rapidly interconvert, even at 213 K on the NMR spectroscopic timescale. Indeed, the interconversion between the two only requires a reversible linear to bent transformation for the  $\text{SCN}^-$  ligands. Similar behavior is observed in the  $^{13}\text{C}\{^1\text{H}\}$  NMR spectra of the mixture of **2a–c**, where only two resonances ( $\delta = 129.8$  ppm and  $\delta = 129.3$  ppm) are observed for the carbon atoms that comprise the  $\text{SCN}^-$  ligands, even at 208 K.

We propose that **2b** is an intermediate in the interconversion of **2a** and **2c** (Scheme 1). The basis for this conclusion comes from analysis of the solid state X-ray crystallographic data, the solution NMR data for the complexes, and DFT calculations (Supporting Information, Figures S6–S8, Table S3). Such calculations suggest that **2b** is higher in energy than **2a** by about  $13 \text{ kcal mol}^{-1}$  and therefore can serve as intermediate in the interconversion of **2a** and **2c**, which is only about  $6.6 \text{ kcal mol}^{-1}$  higher in energy than **2a** (Supporting Information, Table S3). Indeed, the single-crystal X-ray data shows longer nickel–thioether bond distances for **2b** than **2a** (ca.  $0.05 \text{ \AA}$ , Table S1), suggesting weaker Ni–S bonds. With this hypothesis, when the thiocyanate ligands rearrange from bent to linear coordination modes in the conversion of **2a** to **2b**, a concomitant weakening of the Ni–S bonds occurs, preparing for the formation of open complex **2c**. Consistent with the conclusion that **2b** is the intermediate rather than **2a**, DFT calculations suggest greater ring strain in its five-membered chelates (the ligand conformation in **2b** is higher in energy than that of **2a** and **2c** by about  $3.3$  and  $4.0 \text{ kcal mol}^{-1}$ , respectively; Supporting Information, Table S3). Interestingly, the SOMO orbitals of the high-spin **2a** are partially located on the metal center, but those of **2b** are predominantly centered on the  $\text{SCN}^-$  ligands with little nickel center contribution, suggesting that the delocalized electronic character of the metal–ligand interaction may be important to the exchange mechanism (Supporting Information, Figures S6, S7). Complex **2c** is calculated to be low spin, consistent with a square-planar nickel(II) complex.

The thermodynamic parameters for the interconversion of **2a** and **2c** can be determined by the construction of a Van't Hoff plot from the VT  $^{31}\text{P}$  NMR spectroscopic data (Support-

ing Information, Figure S9). From these data, one can conclude that the reaction is enthalpically disfavored ( $\Delta H^\circ = 2.8 \text{ kcal mol}^{-1}$ ) as written but entropically favored ( $\Delta S^\circ = 11.5 \text{ cal mol}^{-1} \text{ K}^{-1}$ ; Scheme 1). This conclusion is consistent with the conversion of a relatively rigid octahedral complex into a more flexible square-planar isomer through two Ni–S bond-breaking processes. At 298 K, the calculated  $\Delta G^\circ$  of this reaction is  $-0.6 \text{ kcal mol}^{-1}$ . The fact that the major product observed when solvent is removed is **2a** can be attributed to the decreased solubility of this product causing a correspondingly more rapid precipitation as the solution becomes more concentrated. The stability of all three species, however, is likely in part the consequence of an energetic barrier between the “open” and “closed” type complexes because of their respective low- and high-spin configurations.<sup>[31,32]</sup> In fact, Evans method measurements of the  $\mu_{\text{eff}}$  values for **2a–c** at 304 K are equal to 2.18 BM (a weighted average of  $S = 1$  for **2a–b** and  $S = 0$  for **2c**), indicating a distribution of both low- and high-spin nickel(II), which is consistent with the broad resonance observed in the  $^{31}\text{P}\{^1\text{H}\}$  NMR spectrum in  $\text{CD}_2\text{Cl}_2$  of the mixture of **2a–c**.<sup>[35,36]</sup> Cooling the sample from room temperature to 195 K shows a linear increase in  $\mu_{\text{eff}}$  values to 3.14 BM ( $S = 1$ ) with a concomitant shift of product distribution towards high-spin, octahedral nickel(II) consistent with previously discussed  $^{31}\text{P}\{^1\text{H}\}$  NMR spectroscopy (Supporting Information, Figures S1 and S9). This result is intuitive based upon the temperature-dependent equilibrium involving high-spin complexes **2a** and **2b** and low-spin complex **2c**. At high temperatures, the equilibrium mixture favors **2c**, decreasing the observed  $\mu_{\text{eff}}$  (Scheme 1). Both **4a** and **4b** were determined to be diamagnetic by the same procedure.

This system is intriguing, since we can isolate three isomers and structurally characterize them. Clearly the barrier to interconversion in the solid state is much greater than in solution, where **2a** and **2b** undergo rapid exchange even at 208 K. This phenomenon seems to be unique to these types of hemilabile ligand complexes formed with  $\text{SCN}^-$  ligands. Indeed, the  $\text{Cl}^-$  versions of these complexes (for example **1** and **3a**) also undergo dynamic exchange in solution (but such processes involve the  $\text{Cl}^-$  ligand moving from the inner to outer coordination sphere); however, only one isomer is ever observed in the solid state.<sup>[29]</sup> The ability of the thiocyanate ligand to adopt multiple coordination modes seems to provide pathways to not only weaken other bonds within the complex but also stabilize other isomers, including the four-coordinate square-planar complex **2c**.

The reason why the interconversion of complexes **2a** and **2c** does not involve the dissociation of the isocyanate ligand similar to the  $\text{Cl}^-$  dissociation event involving **1** most likely involves the higher Ni–N bond strength as compared to Ni–Cl. N-bound  $\text{SCN}^-$  is a much stronger field ligand than  $\text{Cl}^-$  according to the spectrochemical series.<sup>[37]</sup> Consistent with this conclusion, the UV/Vis data show a shift in the d–d transition from 512 nm in **1** to 485 nm in **2a–c** (Supporting Information, Figure S11), which is indicative of a higher-energy transition. Therefore, the only weak metal–ligand interactions in this system are the Ni–S bonds.

These computational and experimental results are consistent with the observed properties of these complexes being directly affected by the presence and nature of Ni–S(R)<sub>2</sub> and Ni–SCN<sup>−</sup> interactions both in solution and the solid state. This interplay has allowed for the unprecedented solid-state characterization of some important species from a bond-breaking isomerization exchange.

Received: October 28, 2011

Revised: November 21, 2011

Published online: December 23, 2011

**Keywords:** bond-breaking isomers · coordination modes · exchange processes · hemilabile ligands · nickel

- [1] E. Poverenov, M. Gandelman, L. J. W. Shimon, H. Rozenberg, Y. Ben-David, D. Milstein, *Organometallics* **2005**, *24*, 1082.
- [2] V. V. Grushin, *Organometallics* **2001**, *20*, 3950.
- [3] P. J. W. Deckers, B. Hessen, J. H. Teuben, *Angew. Chem.* **2001**, *113*, 2584; *Angew. Chem. Int. Ed.* **2001**, *40*, 2516.
- [4] G. L. Moxman, H. E. Randell-Sly, S. K. Brayshaw, R. L. Woodward, A. S. Weller, M. C. Willis, *Angew. Chem.* **2006**, *118*, 7780; *Angew. Chem. Int. Ed.* **2006**, *45*, 7618.
- [5] R. Lindner, B. van der Bosch, M. Lutz, N. H. J. Reek, J. I. van der Vlugt, *Organometallics* **2011**, *30*, 499.
- [6] A. M. Spokoyny, C. W. Machan, D. J. Clingerman, M. S. Rosen, M. J. Wiester, R. D. Kennedy, A. A. Sarjeant, C. L. Stern, C. A. Mirkin, *Nat. Chem.* **2011**, *3*, 590.
- [7] M. S. Rosen, A. M. Spokoyny, C. W. Machan, C. L. Stern, A. A. Sarjeant, C. A. Mirkin, *Inorg. Chem.* **2011**, *50*, 1411.
- [8] O. T. Summerscales, F. G. N. Cloke, P. B. Hitchcock, J. C. Green, N. Hazari, *Science* **2006**, *311*, 829.
- [9] M. D. Fryzuk, W. E. Piers, *Polyhedron* **1988**, *7*, 1001.
- [10] L. Kovbasyuk, R. Kramer, *Chem. Rev.* **2004**, *104*, 3161.
- [11] H. J. Yoon, C. A. Mirkin, *J. Am. Chem. Soc.* **2008**, *130*, 11590.
- [12] M. Takeuchi, M. Ikeda, A. Sugasaki, S. Shinkai, *Acc. Chem. Res.* **2001**, *34*, 865.
- [13] H. J. Yoon, J. Kuwabara, J.-H. Kim, C. A. Mirkin, *Science* **2010**, *330*, 66.
- [14] A. Bader, E. Lindner, *Coord. Chem. Rev.* **1991**, *108*, 27.
- [15] C. S. Slone, D. A. Weinberger, C. A. Mirkin, *Prog. Inorg. Chem.*, **1999**, *48*, 233.
- [16] M. J. Wiester, P. A. Ulmann, C. A. Mirkin, *Angew. Chem.* **2011**, *123*, 118; *Angew. Chem. Int. Ed.* **2011**, *50*, 114.
- [17] P. Braunstein, *J. Organomet. Chem.* **2004**, *689*, 3953.
- [18] C. W. Rogers, M. O. Wolf, *Coord. Chem. Rev.* **2002**, *233–234*, 341.
- [19] Z. Weng, S. Teo, T. S. A. Hor, *Acc. Chem. Res.* **2007**, *40*, 676.
- [20] T. J. M. de Bruin, L. Magna, P. Raybaud, H. Toulhoat, *Organometallics* **2003**, *22*, 3404.
- [21] B. M. Foxman, P. L. Goldberg, H. Mazurek, *Inorg. Chem.* **1981**, *20*, 4368.
- [22] G. Parkin, *Chem. Rev.* **1993**, *93*, 887.
- [23] J. Bernstein, R. J. Davey, J.-O. Henck, *Angew. Chem.* **1999**, *111*, 3646; *Angew. Chem. Int. Ed.* **1999**, *38*, 3440.
- [24] D. Braga, F. Grepioni, *Chem. Soc. Rev.* **2000**, *29*, 229.
- [25] a) D. Braga, L. Maini, M. Polito, L. Scaccianoce, G. Cojazzi, F. Grepioni, *Coord. Chem. Rev.* **2001**, *216–217*, 225; b) J. A. Labinger, *C. R. Chim.* **2002**, *5*, 235.
- [26] a) T. P. Brewster, W. Ding, N. D. Schley, N. Hazari, V. S. Batista, R. H. Crabtree, *Inorg. Chem.* **2011**, *50*, 11938; b) L. E. Hatcher, M. R. Warren, D. R. Allan, S. K. Brayshaw, A. L. Johnson, S. Fuertes, S. Schiffrs, A. J. Stevenson, S. J. Teat, C. H. Woodall, P. R. Raithby, *Angew. Chem.* **2011**, *123*, 8521; *Angew. Chem. Int. Ed.* **2011**, *50*, 8371; c) M. R. Warren, S. K. Brayshaw, A. L. Johnson, S. Schiffrs, P. R. Raithby, T. L. Easun, M. W. George, J. E. Warren, S. J. Teat, *Angew. Chem.* **2009**, *121*, 5821; *Angew. Chem. Int. Ed.* **2009**, *48*, 5711.
- [27] J. Bernstein, *Cryst. Growth Des.* **2011**, *11*, 632.
- [28] P. E. Garrou, *Chem. Rev.* **1981**, *81*, 229.
- [29] C. W. Machan, A. M. Spokoyny, M. R. Jones, A. A. Sarjeant, C. L. Stern, C. A. Mirkin, *J. Am. Chem. Soc.* **2011**, *133*, 3023.
- [30] CCDC 851134 (**4b**), 851135 (**2b**), 851136 (**3a**), 851137 (**2c**), 851138 (**2a**), and 851139 (**4a**) contain the supplementary crystallographic data for this paper. These data can be obtained free of charge from The Cambridge Crystallographic Data Centre via [www.ccdc.cam.ac.uk/data\\_request/cif](http://www.ccdc.cam.ac.uk/data_request/cif).
- [31] U. Kölle, J. Kossakowski, N. Klaff, L. Wesemann, U. Englert, G. E. Heberich, *Angew. Chem.* **1991**, *103*, 732; *Angew. Chem. Int. Ed. Engl.* **1991**, *30*, 690.
- [32] U. Kölle, *Angew. Chem.* **1991**, *103*, 970; *Angew. Chem. Int. Ed. Engl.* **1991**, *30*, 956.
- [33] R. A. Bailey, S. L. Kozak, T. W. Michelsen, W. N. Mills, *Coord. Chem. Rev.* **1971**, *6*, 407.
- [34] J. Coates, *Encyclopedia of Analytical Chemistry* (Ed.: R. A. Meyers), Wiley, Chichester, **2000**, p. 10815.
- [35] G. A. Bain, J. F. Berry, *J. Chem. Educ.* **2008**, *85*, 532.
- [36] E. M. Schubert, *J. Chem. Educ.* **1992**, *69*, 62.
- [37] P. Atkins, T. Overton, J. Rourke, M. Weller, F. Armstrong, *Inorganic Chemistry*, Oxford University Press, Oxford, England, **2006**.